



CHORUS

This is the accepted manuscript made available via CHORUS. The article has been published as:

Charge and spin criticality for the continuous Mott transition in a two-dimensional organic conductor

Michael Sentef, Philipp Werner, Emanuel Gull, and Arno P. Kampf

Phys. Rev. B **84**, 165133 — Published 28 October 2011

DOI: [10.1103/PhysRevB.84.165133](https://doi.org/10.1103/PhysRevB.84.165133)

Charge and spin criticality for the continuous Mott transition in a two-dimensional organic conductor

Michael Sentef,^{1,2,*} Philipp Werner,³ Emanuel Gull,⁴ and Arno P. Kampf¹

¹*Theoretical Physics III, Center for Electronic Correlations and Magnetism,
Institute of Physics, University of Augsburg, D-86135 Augsburg, Germany*

²*Stanford Institute for Materials and Energy Science,
SLAC National Accelerator Laboratory, 2575 Sand Hill Road, Menlo Park, CA 94025, USA*

³*Theoretische Physik, ETH Zurich, 8093 Zürich, Switzerland*

⁴*Department of Physics, Columbia University, New York, NY 10027, USA*

(Dated: October 4, 2011)

We study the continuous bandwidth-controlled Mott transition in the two-dimensional single-band Hubbard model with a focus on the critical scaling behavior of charge and spin degrees of freedom. Using plaquette cluster dynamical mean-field theory, we find charge and spin criticality consistent with experimental results for organic conductors. In particular, the charge degree of freedom calculated via the local density of states at the Fermi level shows a smoother transition than expected for the Ising universality class and in single-site dynamical mean-field theory, revealing the importance of short-ranged nonlocal correlations in two spatial dimensions. The spin criticality obtained from the local spin susceptibility agrees quantitatively with nuclear magnetic resonance measurements of the spin-lattice relaxation rate.

PACS numbers: 71.10.Fd, 71.30.+h, 74.70.Kn

I. INTRODUCTION

The Mott metal-insulator transition (MIT) is a paradigmatic example of a correlation-induced phase transition.¹ Its physics is generically contained in the single-band Hubbard model, which is parametrized by the local Coulomb repulsion U , the bare bandwidth W , and the average electron density n . Two MITs are distinguished: first, the bandwidth-controlled Mott transition at fixed filling, where an insulator turns into a metal by increasing W/U , typically realized in experiments through chemical or hydrostatic pressure, and second the filling-controlled Mott transition at fixed U/W , where the system becomes metallic upon adding electrons or holes. A paramagnetic Mott transition is often superceded by antiferromagnetic ordering unless the system is frustrated or the temperature high enough so that the bandwidth-controlled MIT proceeds from a paramagnetic metal to a paramagnetic insulator. Typically, the paramagnetic MIT is a discontinuous first-order transition at low temperatures with a continuous critical end point.

The scaling behavior at the critical end point, or in short Mott criticality, for the bandwidth-controlled MIT has been probed experimentally for the charge degree of freedom via the dc conductivity, e.g. for $(V_{1-x}Cr_x)_2O_3$ ² or the quasi-two-dimensional κ -(ET)₂Cu[N(CN)₂]Cl (abbreviated as κ -Cl).^{3,4} The latter belongs to a class of layered organic charge transfer salts,^{5,6} which are both low-dimensional and geometrically frustrated, such that magnetic order is suppressed at the temperature of the critical end point of the Mott transition. These organic salts therefore allow to follow the first-order MIT to its second order critical end point in the absence of magnetic long-range order. Only recently Mott criticality was also investigated for the spin degree of freedom by nuclear magnetic resonance (NMR) measurements under pressure.⁷ The focus of the latter study was on the critical scaling behavior upon varying pressure at fixed temperature, which is described by a critical exponent δ . Here we present a theoretical modeling of the spin and charge Mott criticality and determine δ . The spin criticality will be investigated via the local spin susceptibility, which is related directly to the NMR spin-lattice relaxation rate $1/T_1$. For the charge criticality we focus on the local density of states at the Fermi energy.

Experimentally Mott criticality is probed by the scaling behavior of a selected quantity σ (e.g., the conductivity) as a function of external parameters such as the temperature T or the pressure p near the critical end point. Specifically one observes scaling with respect to the reduced parameters $t_{\text{red}} = (T - T_c)/T_c$ and $p_{\text{red}} = (p - p_c)/p_c$, where the index c denotes the values at the critical end point. Criticality is then classified by the set of exponents β , γ , and δ via

$$\begin{aligned} \sigma(t_{\text{red}}, p_{\text{red}} = 0) - \sigma_c &\propto |t_{\text{red}}|^\beta, \\ \left. \frac{\partial \sigma(t_{\text{red}}, p_{\text{red}})}{\partial p_{\text{red}}} \right|_{p_{\text{red}}=0} &\propto |t_{\text{red}}|^{-\gamma}, \\ \sigma(t_{\text{red}} = 0, p_{\text{red}}) - \sigma_c &\propto |p_{\text{red}}|^{1/\delta}, \end{aligned} \quad (1)$$

where $\sigma_c = \sigma(t_{\text{red}} = 0, p_{\text{red}} = 0)$. The critical exponents obey the scaling law $\gamma = \delta(\beta - 1)$.⁸

The Mott transition has been proposed to be in the Ising universality class⁹⁻¹² based on the assumption that the double occupancy may serve as a fingerprint observable for the MIT, which plays a similar role as the order parameter in a thermodynamic phase transition to a broken symmetry state. The universality class of a second-order phase transition is determined by the symmetry of the order parameter and the spatial dimension; the scalar character of the double occupancy would imply the Ising universality class.⁸ Conductivity measurements for $(V_{1-x}Cr_x)_2O_3$ indeed confirm critical behavior compatible with 3D Ising universality ($\beta \approx 0.33$, $\gamma \approx 1.2$, $\delta \approx 4.8$),^{2,8} but the situation for the two-dimensional κ -Cl has remained controversial.

The critical exponents of the 2D Ising model are $\beta = 1/8$, $\gamma = 7/4$, and $\delta = 15$.¹³ Conductivity measurements under pressure performed on κ -Cl challenge the prediction of Ising universality, since the observed exponents are $\beta \approx 1$, $\gamma \approx 1$, and $\delta \approx 2$. Imada *et al.* argued that the observed deviation from Ising universality is a manifestation of unconventional quantum criticality specific to a two-dimensional system.^{14,15} A different scenario was proposed by Papanikolaou *et al.* who claimed that the conductivity can have a different critical behavior than the order parameter of the transition.¹²

In NMR experiments under pressure on κ -Cl Kagawa *et al.* observed that the critical enhancement of the conductivity upon passing through the critical end point is accompanied by a critical suppression of spin fluctuations;⁷ the latter was inferred from a decrease of the nuclear spin-lattice relaxation rate T_1^{-1} . Identical critical exponents δ were determined for the conductivity and the spin relaxation $1/(T_1T)$ within experimental accuracy.

II. MODEL AND METHODS

Here we aim at a microscopic description of Mott criticality in organic conductors by studying the two-dimensional one-band Hubbard model on an anisotropic triangular lattice with the Hamiltonian

$$H = \sum_{\mathbf{k}, \sigma} (\epsilon_{\mathbf{k}} - \mu) c_{\mathbf{k}, \sigma}^\dagger c_{\mathbf{k}, \sigma} + U \sum_i n_{i, \uparrow} n_{i, \downarrow}, \quad (2)$$

where $c_{\mathbf{k}, \sigma}^\dagger$ ($c_{\mathbf{k}, \sigma}$) creates (annihilates) an electron in a Bloch state with lattice momentum \mathbf{k} . $n_{i, \sigma}$ is the local density operator for site i and spin $\sigma = \uparrow, \downarrow$, $U > 0$ is the local Coulomb repulsion strength, and μ is the chemical potential. The electronic dispersion is given by

$$\epsilon_{\mathbf{k}} = -2t(\cos k_x + \cos k_y) - 2t_{\text{diag}} \cos(k_x + k_y). \quad (3)$$

Following Ref. 16 we choose for κ -Cl a diagonal hopping $t_{\text{diag}} = 0.44t$ and fix the filling at $n = 1$ in a grand-canonical calculation.

We obtain an approximate solution of the Hubbard model by using cluster dynamical mean-field theory (CDMFT) on a 2×2 plaquette. The CDMFT self-consistency equations^{17,18} are

$$\mathbf{G}(i\omega_n) = \sum_{\tilde{\mathbf{k}}} \left((i\omega_n + \mu)\mathbf{1} - \boldsymbol{\Sigma}(i\omega_n) - \mathbf{t}(\tilde{\mathbf{k}}) \right)^{-1}, \quad (4)$$

$$\mathcal{G}_0^{-1}(i\omega_n) = \mathbf{G}^{-1}(i\omega_n) - \boldsymbol{\Sigma}(i\omega_n). \quad (5)$$

For the $N_c = 2 \times 2$ plaquette CDMFT, the hopping matrix $\mathbf{t}(\tilde{\mathbf{k}})$ is defined via its matrix elements $t_{ij}(\tilde{\mathbf{k}}) = N_c^{-1} \sum_{\mathbf{k}} e^{i(\mathbf{k} + \tilde{\mathbf{k}}) \cdot (\mathbf{X}_i - \mathbf{X}_j)} \epsilon_{\mathbf{k} + \tilde{\mathbf{k}}}$, where \mathbf{X}_i and \mathbf{X}_j are the position vectors of cluster sites i and j , $\tilde{\mathbf{k}}$ is in the reduced Brillouin zone, and the cluster momenta take the values $\mathbf{k} = (0, 0)$, $(\pi, 0)$, $(0, \pi)$, and (π, π) . All quantities, i.e. \mathbf{t} , the coarse-grained cluster Green function \mathbf{G} , the Weiss field \mathcal{G}_0 , and the cluster self-energy $\boldsymbol{\Sigma}$ are $N_c \times N_c$ matrices, and $\mathbf{1}$ is the unit matrix. In the following we consider only paramagnetic solutions and the spin index is therefore suppressed.

The self-consistency cycle is closed by solving the impurity problem, i.e. by calculating a new cluster Green function matrix $\mathbf{G}_{ij}(\tau) = -\langle \mathcal{T}_\tau c_i(\tau) c_j^\dagger(0) \rangle_{S_{\text{eff}}}$ for a given self-energy and the corresponding Weiss field. Here S_{eff} denotes the effective action of the auxiliary Anderson impurity model, which is solved by numerically exact continuous-time quantum Monte Carlo (QMC) simulations based on the expansion of S_{eff} in the impurity-bath hybridization.¹⁹⁻²¹ In contrast to single-site DMFT,²²⁻²⁴ CDMFT takes short-ranged nonlocal correlations within the cluster into account. These nonlocal correlations are particularly important for two-dimensional systems.²⁵⁻³⁵

We employ the following strategy for obtaining information on the critical behavior at the continuous Mott transition: First, we calculate the double occupancy $D = N_c^{-1} \sum_{i=1}^{N_c} \langle n_{i\uparrow} n_{i\downarrow} \rangle$ as a function of U for a fixed ratio t/T and search for hysteresis, i.e. whether there is a finite U region in which both a metallic and a Mott-insulating solution of the self-consistent CDMFT equations exist depending on the initial guess for the self-energy. If hysteresis occurs, the temperature T is increased, otherwise T is decreased. This procedure is repeated until the boundary between hysteretic and non-hysteretic behavior is determined accurately. The critical inverse temperature for the continuous Mott transition is denoted as $(t/T)_c$; the critical end point is determined by the two parameters $(U/T)_c$ and $(t/T)_c$. Spin and charge criticality are subsequently measured and quantified by

$$\sigma_{ch} = G_{\text{loc}}(1/(2T)), \quad (6)$$

$$\sigma_{sp} = \lim_{\omega \rightarrow 0} \frac{\text{Im } \chi_{\text{loc}}(\omega)}{\omega}, \quad (7)$$

which are both functions of the reduced variables t_{red} and p_{red} .

The local Green function $G_{\text{loc}}(\tau) = N_c^{-1} \sum_{i=1}^{N_c} \langle c_i(\tau) c_i^\dagger \rangle$ measured at imaginary time $\tau = 1/(2T)$ approximates $TA(\omega = 0)$ and thus gives an estimate for the local density of states at the Fermi energy without necessitating an analytical continuation procedure for the imaginary-time data.^{36,37} Therefore σ_{ch} serves as one possible measure for the criticality of the charge degree of freedom. The spin excitation spectrum is reflected in the local dynamical spin susceptibility $\chi_{\text{loc}}(\omega)$, which is calculated by a QMC measurement of the imaginary time correlation function $\chi_{\text{loc}}(\tau) = N_c^{-1} \sum_{i=1}^{N_c} \langle S_{i,z}(\tau) S_{i,z}(0) \rangle$ and the analytic continuation of its Matsubara transform to real frequencies. Here we use the maximum entropy method³⁸ for the bosonic kernel according to

$$\chi_{\text{loc}}(\tau) = \int \frac{d\omega}{\pi} \frac{e^{-\tau\omega}}{1 - e^{-\omega/T}} \text{Im } \chi_{\text{loc}}(\omega). \quad (8)$$

In the Mott insulator $\text{Im } \chi_{\text{loc}}(\omega)/\omega$ is sharply peaked at $\omega = 0$. This behavior prohibits a reliable determination of σ_{sp} in the insulator from our numerical data. We therefore restrict the analysis of spin criticality to the metallic side of the transition.

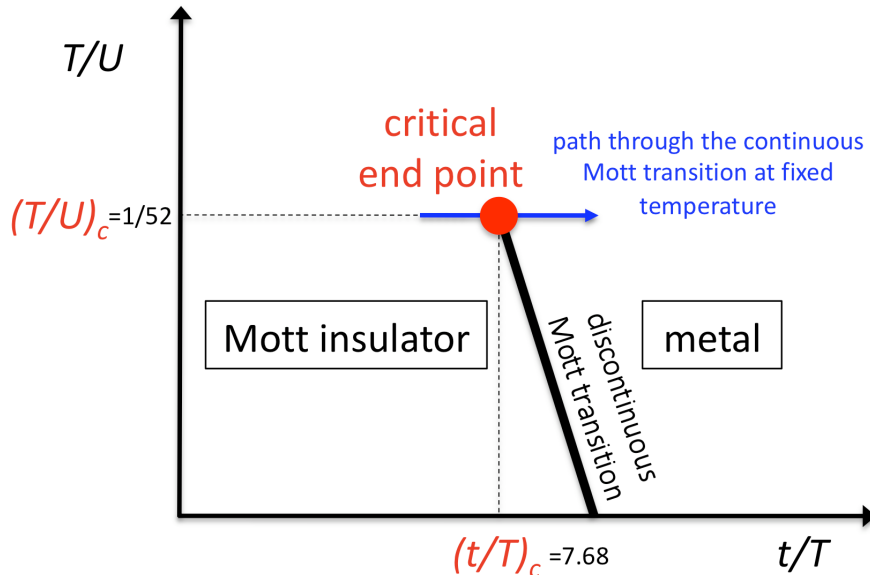


FIG. 1. Schematic path through the continuous Mott transition at fixed temperature. We assume that the pressure-controlled transition in Ref. 7 corresponds approximately to the bandwidth-controlled transition in the Hubbard model. The hopping amplitude t (bandwidth $W \propto t$) is varied (blue arrow) while the local Coulomb repulsion U , the relative anisotropic diagonal hopping t_{diag}/t and the temperature T are kept fixed in our calculations. The indicated values of $(T/U)_c$ and $(t/T)_c$ are the critical values found for $t_{\text{diag}}/t = 0.44$.

In order to model the bandwidth-controlled Mott transition by tuning the pressure, some further assumptions are necessary: We assume that varying t/U amounts to varying pressure, and that T/U is kept fixed at constant temperature. In essence this implies that the value of U is fixed independent of external conditions in the experiment. This is motivated by the fact that the Hubbard interaction is strictly local. Moreover we make the approximation that $t_{\text{diag}}/t = 0.44$ remains fixed at the value taken from a fit to the band structure¹⁶ even when pressure is applied. Fig. 1 summarizes our strategy for modeling the continuous Mott transition across the critical end point.

III. RESULTS

The basis for the discussion of the critical behavior are the data displayed in Fig. 2. Both charge and spin degrees of freedom show critical behavior with an infinite slope at the continuous transition, which is identified at $(t/T)_c = 7.68$, independently for charge and spin. The theoretical results resemble the experimental data for the criticality of the conductivity and the NMR spin-lattice relaxation rate $1/T_1$ in Ref. 7 qualitatively. The increase of $G_{\text{loc}}(1/(2T))$ indicates that the low-energy spectral weight increases upon passing from the insulator to the metal. This behavior reflects the closing and the filling of the charge gap with low-energy states at finite temperatures. Similarly, the measured conductivity will increase in the metal. In contrast, the spin susceptibility behaves oppositely; it is suppressed with increasing “pressure” on the metallic side of the continuous MIT and enhanced in the insulator, as measured by $1/(T_1 T)$.

This qualitative behavior of the spin susceptibility finds a natural interpretation in terms of the probabilities of relevant plaquette eigenstates in the ensemble.³¹ The enhancement of spin fluctuations in the insulator is thereby traced to the predominant occupation of the plaquette with a four-electron singlet state³⁷ with zero total momentum and zero total spin $S = 0$. The second-most probable states are the three triplet states with spin $S = 1$. Since the singlet state has a high occupation probability in the insulator, spin flip ($\Delta S = 1$) excitations to the triplet states are more likely and lead to the large susceptibility in the insulator.

The lower panel of Fig. 2 shows the critical scaling behavior in a double-logarithmic plot of σ_{ch} and σ_{sp} relative to their values at the critical point as a function of $|t/T - (t/T)_c|/(t/T)_c$. From linear fits to the double-logarithmic

plot we extract the critical exponents according to Eq. (1). Error bars are estimated from the linear regression fit to the data in the double-logarithmic scale. For the charge criticality the exponent $1/\delta = 0.58 \pm 0.06$ is obtained on the insulating and $1/\delta = 0.61 \pm 0.05$ on the metallic side of the transition. The critical behavior with an infinite slope of the density of states at the Fermi energy is apparent and resembles the measured dc conductivity.⁴ The virtue of a direct quantitative comparison is, however, uncertain because the conductivity and the density of states at the Fermi energy may follow different scaling laws.¹² For the spin criticality, instead, a comparison is meaningful and the quantitative agreement with experiment is remarkable, with an exponent 0.48 ± 0.03 consistent within error bars with the experimentally determined $1/\delta \approx 0.5$.⁷

TABLE I. Summary of critical exponent δ for various models and experiments.

Model	δ	Ref.
Ising ($D = \infty$)	3	[8]
Ising ($D = 3$)	4.8	[8]
Ising ($D = 2$)	15	[13]
Hubbard (single-site DMFT)	3	[10]
Hubbard (2×2 CDMFT)		
σ_{ch} (ins.)	1.72 ± 0.17	
σ_{ch} (met.)	1.64 ± 0.13	
σ_{sp} (met.)	2.08 ± 0.10	
Experiment	δ	
$(V_{1-x}Cr_x)_2O_3$	≈ 5	[2]
κ -Cl		
conductivity	≈ 2	[7]
NMR $1/(T_1T)$	≈ 2	[7]

Table I summarizes the values of the critical exponent $\delta > 1$ for various theoretical models and for several experiments probing the continuous Mott transition. Note that $\delta \rightarrow 1$ corresponds to a smooth transition with a vanishing discontinuity in the first derivative of σ_{ch} , while $\delta \rightarrow \infty$ describes a discontinuous transition with a discontinuity in σ_{ch} itself.

IV. DISCUSSION

Our results for plaquette CDMFT are consistent with the experimental data for κ -Cl both for the charge and the spin degree of freedom. In particular, the critical exponent δ is much smaller than expected for the Ising universality class in two dimensions ($\delta = 15$) and also smaller than in single-site DMFT ($\delta = 3$). The difference between single-site DMFT and four-site cluster DMFT is indeed striking. The latter includes nonlocal correlations and thereby allows for a coarse momentum-space differentiation. Hence, electrons in parts of the Brillouin zone become localized already in the metallic phase. In contrast to single-site DMFT, where the Mott transition occurs simultaneously by a loss of quasiparticle integrity along the whole Fermi surface, the Fermi surface itself may disintegrate and ultimately vanish at the Mott transition within cluster DMFT.²⁹ Therefore, only a smaller fraction of electrons indeed exhibits critical behavior, which is why the transition is smoother (translating into a smaller value of δ) than in single-site DMFT. We point out that the explanation of the observed criticality in terms of momentum-space differentiation was proposed in Ref. 39, in which the critical behavior is suggested to be a finite-temperature manifestation of a marginal quantum critical point.

Regarding the discrepancy between 2×2 CDMFT and single-site DMFT results, we remark that convergence with cluster size may not have been reached, and quantitative corrections to our results may be expected on larger clusters. We stress, however, that both quantities on which we focused in this work are local quantities, which should depend less strongly on the cluster size than nonlocal quantities which probe spatial ordering correlations such as, for example, order parameter susceptibilities or ordering temperatures. A quantitative scaling analysis as a function of cluster size is computationally demanding and beyond the scope of the present study. Resolving this issue would be an interesting subject for future research.

We acknowledge discussions with Fumitaka Kagawa, Kazushi Kanoda, Rafael Fernandes, and Masatoshi Imada. M.S. and A.P.K. are supported by the DFG through TRR 80. M.S. acknowledges support by the Studienstiftung des Deutschen Volkes, E.G. by NSF-DMR-1006282, and P.W. by SNF grant PP001-118866. Computer simulations were performed on HLRB II at LRZ Garching using a code based on the ALPS libraries.⁴⁰

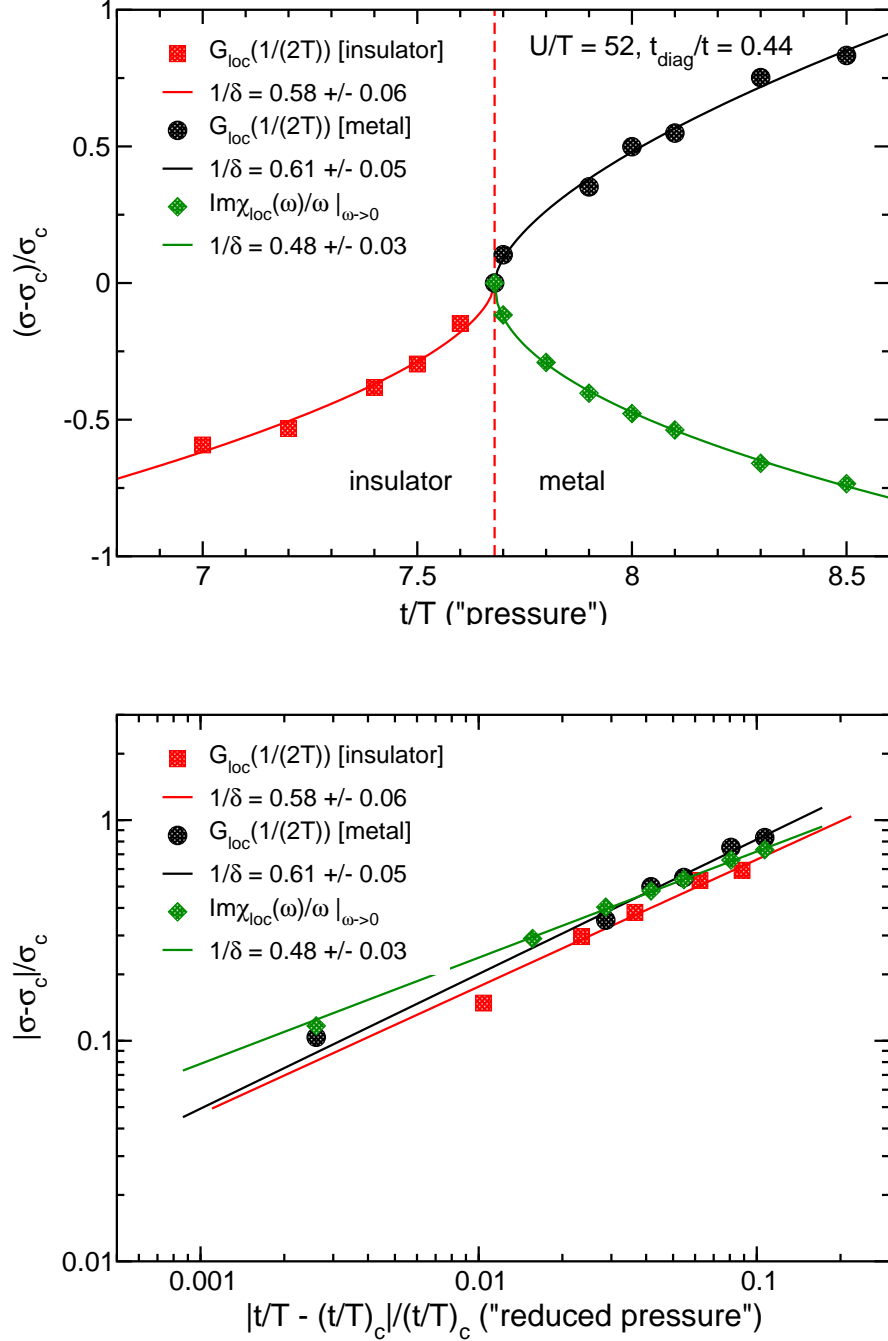


FIG. 2. Critical behavior at the continuous bandwidth-controlled Mott transition (vertical dashed line, $(T/t)_c = 7.68$). Upper panel: Evolution of $(\sigma_{ch} - \sigma_{c,ch})/\sigma_{c,ch}$ and $(\sigma_{sp} - \sigma_{c,sp})/\sigma_{c,sp}$ upon increasing t/T . The solid curves are fits to the critical scaling behavior for the exponent δ according to Eq. (1). Lower panel: Double-logarithmic plot of the same data measured from the critical end point of the Mott transition. Solid lines show the scaling fits (the same fits as in the upper panel). Error bars are estimated from the linear regression fit to the data in the double-logarithmic scale.

-
- * sentefmi@physik.uni-augsburg.de
- ¹ M. Imada, A. Fujimori, and Y. Tokura, *Rev. Mod. Phys.* **70**, 1039 (1998).
 - ² P. Limelette, A. Georges, D. Jérôme, P. Wzietek, P. Metcalf, and J. M. Honig, *Science* **302**, 89 (2003).
 - ³ P. Limelette, P. Wzietek, S. Florens, A. Georges, T. A. Costi, C. Pasquier, D. Jérôme, C. Mézière, and P. Batail, *Phys. Rev. Lett.* **91**, 016401 (2003).
 - ⁴ F. Kagawa, K. Miyagawa, and K. Kanoda, *Nature* **436**, 534 (2005).
 - ⁵ H. Kino and H. Fukuyama, *J. Phys. Soc. Jpn.* **65**, 2158 (1996).
 - ⁶ M. Dumm, D. Faltermeier, N. Drichko, M. Dressel, C. Mézière, and P. Batail, *Phys. Rev. B* **79**, 195106 (2009).
 - ⁷ F. Kagawa, K. Miyagawa, and K. Kanoda, *Nature Phys.* **5**, 880 (2009).
 - ⁸ N. Goldenfeld, *Lectures on Phase Transitions and the Renormalization Group* (Addison-Wesley, Boston, 1992).
 - ⁹ C. Castellani, C. DiCastro, D. Feinberg, and J. Ranninger, *Phys. Rev. Lett.* **43**, 1957 (1979).
 - ¹⁰ G. Kotliar, E. Lange, and M. J. Rozenberg, *Phys. Rev. Lett.* **84**, 5180 (2000).
 - ¹¹ S. Onoda and N. Nagaosa, *J. Phys. Soc. Jpn.* **72**, 2445 (2003).
 - ¹² S. Papanikolaou, R. M. Fernandes, E. Fradkin, P. W. Phillips, J. Schmalian, and R. Sknepnek, *Phys. Rev. Lett.* **100**, 026408 (2008).
 - ¹³ B. M. McCoy and T. T. Wu, *The Two-Dimensional Ising Model* (Harvard University, Cambridge, 1973).
 - ¹⁴ M. Imada, *Phys. Rev. B* **72**, 075113 (2005).
 - ¹⁵ M. Imada, T. Misawa, and Y. Yamaji, *J. Phys. Condens. Matter* **22**, 164206 (2010).
 - ¹⁶ H. C. Kandpal, I. Opahle, Y.-Z. Zhang, H. O. Jeschke, and R. Valentí, *Phys. Rev. Lett.* **103**, 067004 (2009).
 - ¹⁷ G. Kotliar, S. Y. Savrasov, G. Palsson, and G. Biroli, *Phys. Rev. Lett.* **87**, 186401 (2001).
 - ¹⁸ T. A. Maier, M. Jarrell, T. Pruschke, and M. H. Hettler, *Rev. Mod. Phys.* **77**, 1027 (2005).
 - ¹⁹ P. Werner, A. Comanac, L. de' Medici, M. Troyer, and A. J. Millis, *Phys. Rev. Lett.* **97**, 076405 (2006).
 - ²⁰ P. Werner and A. J. Millis, *Phys. Rev. B* **74**, 155107 (2006).
 - ²¹ E. Gull, A. J. Millis, A. I. Lichtenstein, A. N. Rubtsov, M. Troyer, and P. Werner, *Rev. Mod. Phys.* **83**, 349 (2011).
 - ²² W. Metzner and D. Vollhardt, *Phys. Rev. Lett.* **62**, 324 (1989).
 - ²³ A. Georges and G. Kotliar, *Phys. Rev. B* **45**, 6479 (1992).
 - ²⁴ M. Jarrell, *Phys. Rev. Lett.* **69**, 168 (1992).
 - ²⁵ A. I. Lichtenstein and M. I. Katsnelson, *Phys. Rev. B* **62**, R9283 (2000).
 - ²⁶ T. D. Stanescu and G. Kotliar, *Phys. Rev. B* **70**, 205112 (2004).
 - ²⁷ O. Parcollet, G. Biroli, and G. Kotliar, *Phys. Rev. Lett.* **92**, 226402 (2004).
 - ²⁸ T. A. Maier, M. Jarrell, T. C. Schulthess, P. R. C. Kent, and J. B. White, *Phys. Rev. Lett.* **95**, 237001 (2005).
 - ²⁹ A. Macridin, M. Jarrell, T. A. Maier, P. R. C. Kent, and E. D'Azevedo, *Phys. Rev. Lett.* **97**, 036401 (2006).
 - ³⁰ B. Kyung and A.-M. S. Tremblay, *Phys. Rev. Lett.* **97**, 046402 (2006).
 - ³¹ K. Haule, *Phys. Rev. B* **75**, 155113 (2007).
 - ³² T. Ohashi, T. Momoi, H. Tsunetsugu, and N. Kawakami, *Phys. Rev. Lett.* **100**, 076402 (2008).
 - ³³ S. Sakai, Y. Motome, and M. Imada, *Phys. Rev. Lett.* **102**, 056404 (2009).
 - ³⁴ A. Liebsch, H. Ishida, and J. Merino, *Phys. Rev. B* **79**, 195108 (2009).
 - ³⁵ G. Sordi, K. Haule, and A.-M. S. Tremblay, *Phys. Rev. Lett.* **104**, 226402 (2010).
 - ³⁶ N. Trivedi and M. Randeria, *Phys. Rev. Lett.* **75**, 312 (1995).
 - ³⁷ E. Gull, P. Werner, X. Wang, M. Troyer, and A. J. Millis, *Europhys. Lett.* **84**, 37009 (2008).
 - ³⁸ M. Jarrell and J. E. Gubernatis, *Phys. Rep.* **269**, 133 (1996).
 - ³⁹ T. Misawa and M. Imada, *Phys. Rev. B* **75**, 115121 (2007).
 - ⁴⁰ A. Albuquerque et al., *J. Magn. Magn. Mater.* **310**, 1187 (2007).